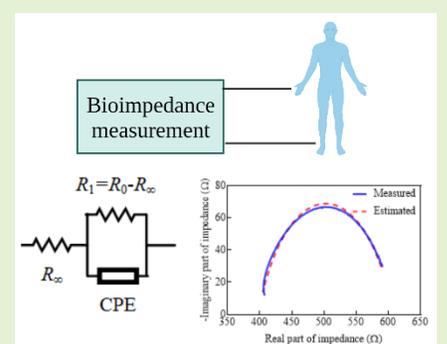


Parameter Estimation of the Single-Dispersion Fractional Cole-Impedance Model with the Embedded Hardware

Mitar Simić, Todd J. Freeborn, Mladen Veletić, Fernando Seoane, and Goran M. Stojanović

Abstract— Bioimpedance modeling with equivalent electrical circuits has an important role in various biomedical applications, as it facilitates understanding of underlying physical and electrochemical processes in applications such as body composition measurements and assessment of clinical conditions. However, estimation of model parameter values is not a straightforward task, especially when complex circuits with fractional-order components (e.g. constant phase elements) are used. In this paper, we propose a low-complexity method for parameter estimation of the Cole-impedance model suitable for low-cost embedded hardware (e.g. 8-bit microcontrollers). Our approach uses only the measured real and imaginary impedance, without any specific software package/toolbox, or initial values provided by the user. The proposed method was validated with synthetic (noiseless and noisy) data and experimental right-side, hand-to-foot bioimpedance data from a healthy adult participant. Moreover, the proposed method was compared in terms of accuracy with the recently published relevant work and commercial Electrical Impedance Spectroscopy software (Bioimp 2.3.4). The performance evaluation in terms of complexity (suitable for deployment for the microcontroller-based platform with 256 kB of RAM and 16 MHz clock speed), execution time (18 seconds for dataset with 256 points) and cost (<25 USD) confirms the proposed method in regards to reliable bioimpedance processing using embedded hardware.

Index Terms— Bioimpedance, Cole equation, estimation, equivalent circuits, fractional-order circuits.



I. INTRODUCTION

BIOIMPEDANCE is usually defined as the electrical impedance of biological cells and tissues [1]. The measurement of tissue bioimpedance has numerous biomedical applications that include the detection of muscle contraction [2], body composition analysis [3], respiration monitoring [4], [5] knee joint health observation [6], and ankle edema assessment [7]. Moreover, bioimpedance is also used for monitoring and detection cell morphological changes of liver tissues [8], blood glucose monitoring [9], and cell proliferation rate assessment [10].

To support biomedical applications, measured bioimpedance data is evaluated by comparing the modulus and/or phase angle changes at discrete frequencies collected from tissues in different conditions (e.g. contracted and relaxed skeletal muscle). Another analysis approach is based on the use of

equivalent electrical circuits to represent the tissue impedance over a range of frequencies. This approach aims to connect the tissue bioimpedance to underlying physical and electrochemical processes represented by electrical components (e.g. resistors, capacitors, constant phase elements). For example, a widely used equivalent electrical circuit for modelling of the electrical impedance of biological cells is composed of three lumped elements in a 2R-1C arrangement. In this arrangement the resistors model extracellular and intracellular liquids and the capacitor models the cell membrane dielectric properties [11]. However, many experimental studies have shown that the simple 2R-1C model is not able to accurately fit bioimpedance data but replacing the capacitor with a constant phase element (CPE) improves the model fit [12], [13], [14], [15]. The 2R-1C equivalent circuit model when the capacitor is replaced with a CPE is given in Fig. 1. This circuit is the electrical representation of the Cole

This research was funded through the European Union's Horizon 2020 research and innovation programme under grant agreement No. 854194. *Corresponding author: Mitar Simić.*

Mitar Simić and Goran M. Stojanović are with the Faculty of Technical Sciences, University of Novi Sad, 21000 Novi Sad, Serbia (e-mails: mitar.simic@uns.ac.rs, sgoran@uns.ac.rs).

Todd J. Freeborn is with the Department of Electrical and Computer Engineering, The University of Alabama, Box 870286, Tuscaloosa, AL, 35487, USA (e-mail: tjfreeborn1@eng.ua.edu).

Mladen Veletić is with the Dept. of Electronic Systems, Norwegian University of Science and Technology 7491 Trondheim, Norway and The Intervention Centre, Technology and Innovation Clinic, Oslo University Hospital 0372, Oslo, Norway (e-mail: mladen.veletic@ntnu.no).

Fernando Seoane is with the Karolinska Institutet, the Karolinska University Hospital and the University of Borås, Sweden (e-mail: fernando.seoane@ki.se).

impedance equation, defined by Kenneth S. Cole in 1940 [16].

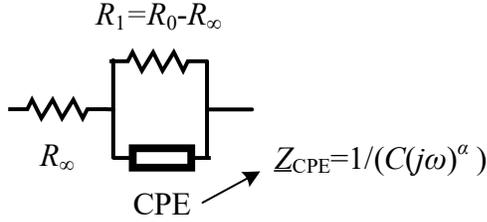


Fig. 1. The equivalent electrical circuit of the Cole-impedance model.

Referring to Fig. 1, note that the Cole-impedance model includes a constant phase element (CPE). This is an element which has a current-voltage relationship described by a fractional-order (α) differential equation [17]. As a result, the Cole-impedance model is dependent on both frequency and the fractional-order. Solving for the parameters of the Cole-impedance model is not a straightforward task and is usually achieved using complex non-linear least squares (NLLS) methods [12], [18], [19], [14], meta-heuristic optimization algorithms (Flower Pollination Algorithm and Moth-Flame Optimizer) [20], fast spectral measurement and regularization [21], or least absolute deviation method [22]. One approach uses the fractional operational matrix for estimating the CPE parameters using a time-domain fitting method. This eliminates the need for impedance measurements, but requires finite-difference time-domain analysis, which requires computation of convolutional integrals or discretization of rational/polynomial functions [23]. Each of the methods described in the above mentioned references are iterative and mostly available within specific software packages (for example MATLAB/Python), or require certain toolboxes (e.g. SciPy for Python). These numerical approaches typically require that an initial value is provided by the user which is iterated upon to find the Cole-impedance parameters that best represent the bioimpedance dataset. In these cases, the accuracy, execution time and convergence are dependent on the quality of the initial values provided by the user. Another limitation of these numerical approaches is that they require a personal computer (PC)-based configuration for deployment, which increases overall price, complexity and reduces the possibility for in-situ applications. While successful deployment and accurate Cole-impedance parameter estimation has been achieved with embedded hardware (e.g. Raspberry Pi 3 platform [18]), the use of lower-performance hardware has the opportunity to further reduce costs associated with bioimpedance instrumentation and its processing. The recently published embedded hardware-based approaches for the parameter estimation of the equivalent electrical circuits were limited to non-fractional models, such as Randles circuit [24], [25].

The main goal of this paper is to advance state of the art with a Cole-impedance parameter estimation method that does not require specific software toolboxes/packages or initial values provided by the user. The estimation method is validated experimentally using a low-cost, 8-bit embedded system using

both simulated and experimental bioimpedance data.

II. METHODS

A. Cole-impedance model and its application in body composition analysis

The complex impedance of the Cole-impedance model (Fig. 1) is given by:

$$\underline{Z}(\omega) = R(\omega) + jX(\omega) = R_\infty + \frac{R_0 - R_\infty}{1 + (R_0 - R_\infty)C(j\omega)^\alpha} \quad (1)$$

where $R(\omega)$ is the real part of the impedance, $X(\omega)$ is the imaginary part of the impedance, and R_∞ , R_0 , C and α are the Cole-impedance model parameters. R_∞ and R_0 are resistances at zero and infinite frequency. These two parameters are also very important for clinical applications, such as body composition analysis (total-body water, body mass index, intracellular/extracellular fluid, *etc.*) [26]. At zero frequency the current flows only through the extracellular fluid, as the cell membrane acts as an insulator, therefore body impedance is described with the parameter R_0 . However, at infinite frequency, the cell membrane acts as a short circuit, the current flows through the intracellular and extracellular fluid, which is identified with the parameter R_∞ . While the exact values of the other two parameters (C and α) are often not used for body composition analysis, they do provide insight into the of relaxation constant $\tau = [(R_0 - R_\infty)C]^{1/\alpha}$ and consequently the characteristic angular frequency $\omega_c = 1/\tau$ of the model. The characteristic frequency ($f_c = \omega_c / (2\pi)$) has been explored to improve the accuracy of total body water estimation [27]. Therefore, the three parameters of most importance for bioimpedance analysis focused on body composition applications are R_0 , R_∞ and f_c . To simplify the notation in this work, we will use $R_1 = R_0 - R_\infty$. This is common in bioimpedance analysis [28] as it simplifies the complexity of equations, which is particularly useful in our proposed method for parameter estimation (Section II.C).

B. Motivation for the development of the new estimation method

There are two measured electrical quantities (R and X) at each discrete bioimpedance measurement at an angular frequency ω . To quantify differences in bioimpedance measurements collected at different timepoints (and potentially representing different physiological states) or from different subjects, the discrete set of measurements are used to estimate the Cole-impedance parameters that best fit the measured data. This has the benefit of reducing the dimensionality of datasets prior to their use and association with underlying physiology or electrochemical processes for bioimpedance analysis.

Some of the Cole parameters can be estimated by graphical analysis of the data in a Nyquist plot. For example, at very low frequency (theoretically ω should be zero), impedance of the Cole impedance model is purely resistive and equal to $R_\infty + R_1$. At very high frequency ($\omega \rightarrow \infty$), a capacitor can be treated as a short circuit, therefore the total impedance is equal to R_∞ . However, the low and high frequency measurements do not provide enough information to estimate all four model parameters which requires measurement of additional

intermediate frequencies. In addition to the theoretical requirements of frequencies to measure, measurements from very low frequencies (typically <10 Hz) to very high frequencies (>100 MHz) are not easily achieved without bulky and costly equipment, which limits their practical measurement. However, a filter-based measurement technique which makes possible estimation of the Cole-model parameters without impedance measurement was reported [15], but it is based on the DC and high frequency gain measurements while also requiring numerically solving of a non-linear equation for parameter α .

C. Proposed estimation method

The main objective of our work is to formulate a method for the Cole-impedance model parameter estimation that uses only the measured resistance and reactance, without needing any specific software toolboxes/packages or initial values provided by the user. Moreover, the proposed solution is optimized for deployment on low-cost microcontroller-based hardware platforms. This is intended to reduce the processing requirements to integrate bioimpedance analysis within embedded hardware.

The proposed estimation method begins with the decomposition of $(j\omega)^\alpha$ to:

$$(j\omega)^\alpha = \omega^\alpha \cos \frac{\alpha\pi}{2} + j\omega^\alpha \sin \frac{\alpha\pi}{2} = a(\omega) + jb(\omega) \quad (2)$$

which shows that for a set of discrete angular frequencies $(\omega_1, \omega_2, \dots, \omega_N)$ a matrix of values $(a_{i,j}, b_{i,j})$ can be calculated for a given value of α . Note, that the parameter α is limited to the range between 0 and 1, and that for a defined number of α -steps (M), the matrix will have $2M$ rows and $N+1$ columns. A representation of this matrix is given in Table I.

TABLE I

THE MATRIX OF (a,b) PAIRS CALCULATED USING EQ. (2) FOR M DIFFERENT VALUES OF α .

		Value of α	Calculated values of (a,b) pairs on frequencies from ω_1 to ω_N for the specific value of α			
2M rows	α_1	$a_{1,1}(\omega_1, \alpha_1)$	$a_{1,2}(\omega_2, \alpha_1)$...	$a_{1,N}(\omega_N, \alpha_1)$	
	α_1	$b_{1,1}(\omega_1, \alpha_1)$	$b_{1,2}(\omega_2, \alpha_1)$...	$b_{1,N}(\omega_N, \alpha_1)$	
	α_2	$a_{2,1}(\omega_1, \alpha_2)$	$a_{2,2}(\omega_2, \alpha_2)$...	$a_{2,N}(\omega_N, \alpha_2)$	
	α_2	$b_{2,1}(\omega_1, \alpha_2)$	$b_{2,2}(\omega_2, \alpha_2)$...	$b_{2,N}(\omega_N, \alpha_2)$	
	
	α_M	$a_{M,1}(\omega_1, \alpha_M)$	$a_{M,2}(\omega_2, \alpha_M)$...	$a_{M,N}(\omega_N, \alpha_M)$	
	α_M	$b_{M,1}(\omega_1, \alpha_M)$	$b_{M,2}(\omega_2, \alpha_M)$...	$b_{M,N}(\omega_N, \alpha_M)$	
	N+1 columns					

After substitution of Eq. (2) into the Cole-impedance given by Eq. (1), the real (or resistive) component $R(\omega)$ becomes:

$$R(\omega) = R_\infty + \frac{R_1(1 + aR_1C)}{(1 + aR_1C)^2 + (bR_1C)^2} \quad (3)$$

while the imaginary (or reactive) component $X(\omega)$ is:

$$X(\omega) = \frac{-bR_1^2C}{(1 + aR_1C)^2 + (bR_1C)^2} \quad (4)$$

The characteristic angular frequency ω_c of the equivalent circuit of the Cole-impedance model shown in Fig. 1, is equal to the reciprocal value of the time constant, given by:

$$\omega_c = \frac{1}{(R_1C)^{1/\alpha}} \quad (5)$$

By substituting $\omega = \omega_c$ in Eq. (3), it becomes:

$$R(\omega = \omega_c) = R_c = R_\infty + \frac{R_1}{2} \quad (6)$$

which is frequency-independent and α -independent. To estimate the characteristic angular frequency from the measured dataset requires that sufficient discrete measurements are collected such that the frequency with maximum reactance, $X(\omega_c)$, can be identified and used to estimate $R_c = R(\omega = \omega_c)$.

Therefore, using equations (3), (4) and (6) with the a and b values in the given frequency range for a fixed α , it is possible to solve for the Cole-impedance parameters at each measurement frequency (ω_i) ,

The model parameter R_∞ is given by:

$$R_\infty(\omega_i) = R_c + (aX(\omega_i) - (b^2R^2(\omega_i) - 2R(\omega_i)R_c b^2 + R_c^2 b^2 + a^2X^2(\omega_i) + b^2X^2(\omega_i)^{1/2})/b) \quad (7)$$

The model parameter R_1 is given by:

$$R_1(\omega_i) = -(2aX(\omega_i) - 2(b^2R^2(\omega_i) - 2b^2R(\omega_i)R_c + b^2R_c^2 + a^2X^2(\omega_i) + b^2X^2(\omega_i)^{1/2})/b) \quad (8)$$

The model parameter C is given by:

$$C(\omega_i) = ((bR_c - bR(\omega_i) + aX(\omega_i))(bR_c + aX(\omega_i) - (b^2R^2(\omega_i) - 2b^2R_cR(\omega_i) + b^2R_c^2 + a^2X^2(\omega_i) + b^2X^2(\omega_i)^{1/2})/(2bX(\omega_i)(a^2 + b^2)(R^2(\omega_i) - 2R(\omega_i)R_c + R_c^2 + X^2(\omega_i))) - (b^2R^2(\omega_i) - 3b^2R(\omega_i)R_c - 2abR(\omega_i)X(\omega_i) + 2b^2R_c^2 + 3abR_cX(\omega_i) + 2a^2X^2(\omega_i) + b^2X^2(\omega_i)^{1/2})/(2bX(\omega_i)(a^2 + b^2)(R^2(\omega_i) - 2R(\omega_i)R_c + R_c^2 + X^2(\omega_i)))) \quad (9)$$

Finally, the unique set of estimated Cole-impedance model parameters is obtained as the mean of arrays $R_\infty(i)$, $R_1(i)$ and $C(i)$, given by Eq. (7)-(9), respectively.

Equations (7)-(9) are calculated for each value of α in range [0,1] with defined step $\Delta\alpha$. As reference values of model parameters are mostly not available, as a criterion for choice of α , we propose the minimum sum of mean relative error for estimated real part of impedance ($R_{est}(\alpha, \omega_i)$) and imaginary part of impedance ($X_{est}(\alpha, \omega_i)$):

$$\arg \min_{\alpha} \left\{ \frac{1}{N} \sum_{i=1}^N \left| \frac{R_{est}(\alpha, \omega_i) - R(\omega_i)}{R(\omega_i)} \right| + \frac{1}{N} \sum_{i=1}^N \left| \frac{X_{est}(\alpha, \omega_i) - X(\omega_i)}{X(\omega_i)} \right| \right\} \quad (10)$$

A typical plot of the sum of mean relative errors, calculated using Eq. (10), for different values of α is shown in Fig. 2.

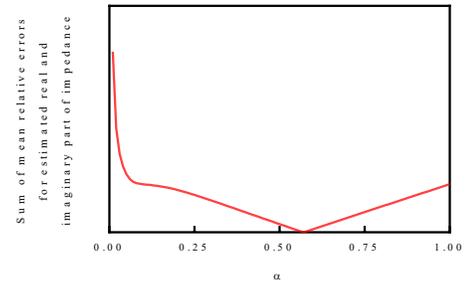


Fig. 2. Plot of mean relative error calculated with Eq. (10) for different values of α .

The impact of the characteristic frequency on the estimation accuracy is determined with the following analysis. The largest absolute error in characteristic frequency estimation is equal to half of the frequency step, as shown in Fig. 3. Assuming that the characteristic frequency is between the frequency points labelled f_k and f_{k+1} in Fig. 4 then the maximum relative error in

characteristic frequency estimation, RE_{f_c} , occurs for the cases when $f_c = f_k + (f_{k+1} - f_k)/2$ and $\Delta f_c = 0.5(f_{k+1} - f_k)$. The maximum relative error can then be determined as:

$$RE_{f_c} = \frac{\Delta f_c}{f_c} = \frac{(f_{k+1} - f_k)/2}{f_k + (f_{k+1} - f_k)/2} = \frac{f_{k+1} - f_k}{f_{k+1} + f_k} \quad (11)$$

The actual relative error will be smaller if the characteristic frequency is closer than a half of the frequency step to some measurement frequency.

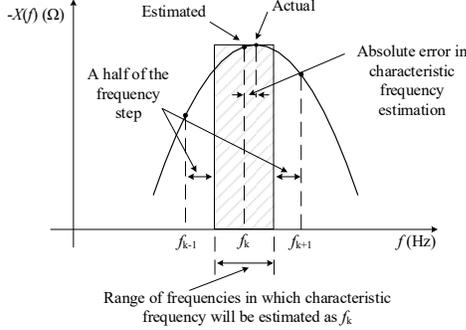


Fig. 3. Characteristic frequency estimation.

The flowchart that outlines each of the steps in the proposed method is shown in Fig. 4.

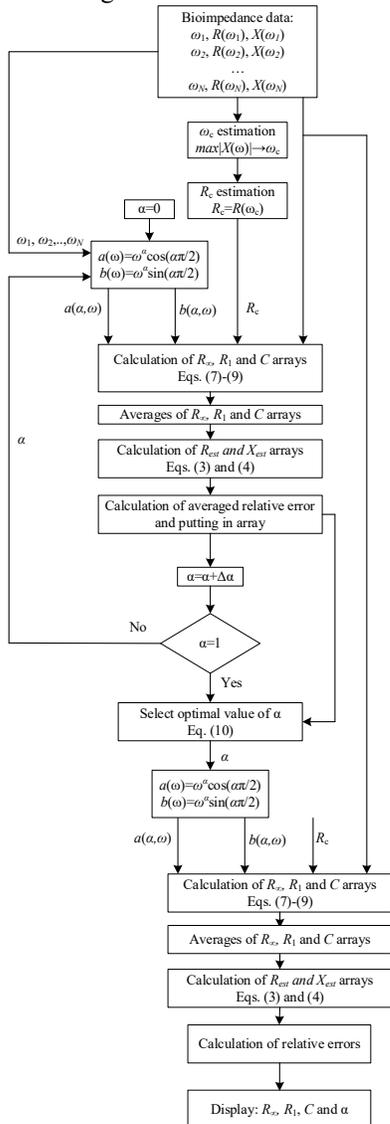


Fig. 4. The flowchart of the proposed method.

In cases using linear frequency steps, the relative error will be higher at lower frequencies. One approach to reduce this error is to decrease the size of the frequency step and measure a greater number of frequencies. However, this approach will increase the overall measurement time and may increase complexity of the required hardware to implement smaller step sizes and store/process a larger number of measurements. Therefore, our approach will use a logarithmic frequency distribution to ensure constant relative error across the complete frequency range. Fig. 5 shows the maximum relative errors calculated using Eq. (11) for linear and logarithmic sweeps across the frequency range from 3 kHz to 1 MHz with 256 discrete points. Notice the linear sweep has a higher maximum relative error below approximately 5 kHz, supporting the earlier discussion.

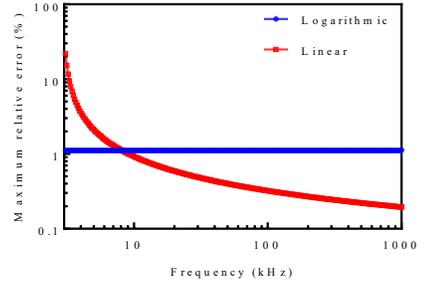


Fig. 5. The maximum relative errors in cases of linear and logarithmic frequency distribution.

The advantage of the proposed method is its low-complexity because all estimation steps include algebraic equations and not the implementation of a complex optimization algorithm. The limitation of the proposed method is the requirement that the characteristic frequency should be included in the frequency range. However, for many biomedical applications the characteristic frequency is in the range of few tens of kHz [15], [27], [29]. For example, a study of 73 healthy adults reported that men in the study had lower characteristic frequency (around 57 kHz) compared to women in the study (around 80 kHz), but men had smaller standard deviation [30], [31]. Most commercial bioimpedance analyzers can measure impedances in the frequency range from a few kHz up to several MHz, so it is reasonable to expect that our methods requirement to capture the characteristic frequency will not present a practical challenge. Beyond, body composition applications the Cole-impedance model has been used in applications to characterize localized tissues and monitor tissue alterations. As an example, impedance measurements of localized biceps tissues of healthy adults before/after exercise from 10 kHz to 100 kHz were reported Freeborn and Fu in [32] and [33]. They reported decreases of R_∞ and R_1 after exercise to exhaustion (e.g. participants were unable to repeat the activity) while C and α did not change significantly [32]. In addition to the decrease of resistive parameters (R_∞ and R_1), after exercise, increases of C were reported at timepoints 72 h and 96 h after the eccentric exercise stimulus (expected to have induced reversible muscle damage) [33]. In addition to these works, a characterization of *ex-vivo* tissues as a function of degradation time has also used the single dispersion Cole-impedance model [34].

It is important to note that not all biological tissues are well modeled by the Cole-impedance model and that higher-complexity models (such as double-dispersion models) may be required for some applications. While the use of a different model excludes this method from being used for those cases, future work should explore parameter estimation techniques using other models (such as the double-dispersion Cole-impedance).

III. RESULTS AND DISCUSSION

A. Parameter estimation using synthetic datasets

To evaluate the performance of the proposed method, parameter estimation was initially applied to a synthetic noiseless impedance dataset generated using reference values: $R_\infty=84.40 \Omega$, $R_1=39.20 \Omega$, $C=2.31 \mu\text{F}$ and $\alpha=0.747$. The corresponding characteristic frequency is $f_c=41.16 \text{ kHz}$. In addition to the noiseless dataset, a noisy dataset with 0.25% random noise was also created. For this dataset, a frequency range of 3 kHz to 1 MHz composed of 256 logarithmically spaced points was used. The frequency range and number of datapoints aligns with datasets previously reported in [18], as well as with the experimental setup used in later sections.

Despite the fact that our estimation method is not platform dependent, and does not require any specific software package or toolbox, it has been implemented here in MATLAB to support further adoption and investigation by other researchers. Specifically, it was using MATLAB2013b deployed on a Dell G5 laptop (Core i7 9th generation). The estimated parameter values using the proposed estimation method with $\Delta\alpha=0.01$ applied to the noiseless dataset are summarized in Table II. These values show very good agreement with their ideal values and a comparison of measured and estimated impedance simulations using ideal and estimated parameters is given in Fig. 6(a). In order to determine the stability of the estimated values as well as the overall execution time, the procedure was repeated 10 times. Estimated values did not change across any of these repeated executions, while average execution time was 105.7 ms with standard deviation of 2.3 ms. Actual values ranged from 103.6 ms to 110.4 ms, indicating good repeatability of the execution time.

To evaluate how the addition of noise impacts the extracted model parameters, the proposed method was applied to the noisy data. This yielded the estimated Cole-impedance parameters summarized in Table II. The comparison of measured and estimated impedance values is given in Fig. 6(b).

TABLE II

ESTIMATED VALUES OF COLE-IMPEDANCE MODEL USING NOISELESS AND NOISY DATASET.

Noiseless dataset						
	$R_\infty (\Omega)$	$R_1 (\Omega)$	$R_0 (\Omega)$	$C (\mu\text{F})$	α	$f_c (\text{kHz})$
Reference	84.40	39.20	123.60	2.31	0.747	41.16
Estimated	84.45	39.07	123.52	2.23	0.75	41.25
RE (%)	0.06%	0.32%	0.06%	3.52%	0.40%	0.22%
Noisy dataset (noise level: 0.25%)						
	$R_\infty (\Omega)$	$R_1 (\Omega)$	$R_0 (\Omega)$	$C (\mu\text{F})$	α	$f_c (\text{kHz})$
Reference	84.40	39.20	123.60	2.31	0.747	41.16
Estimated	84.23	39.06	123.29	2.20	0.75	42.01
RE (%)	0.20%	0.37%	0.25%	4.78%	0.40%	2.06%

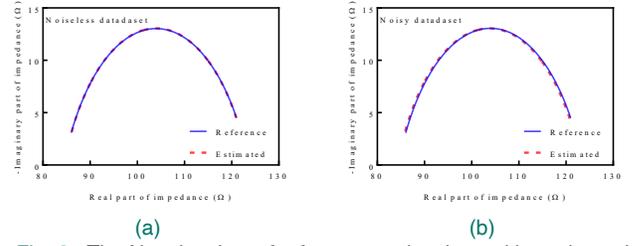


Fig. 6. The Nyquist plots of reference and estimated impedance in case of (a) noiseless and (b) noisy dataset.

As it can be seen from Tables II, as well as Fig. 6, the proposed method provided estimated parameters that showed strong agreement with the ideal parameters used to generate the datasets. The relative errors (RE) in estimation of the three most important parameters (R_0 , R_∞ and f_c) are lower than 2.06% and 0.22% in case of the noisy and noiseless datasets, respectively. The differences in accuracy are attributed to the impact of the dataset noise on the estimation of the characteristic frequency and R_c , which influences the calculation of the Cole model parameters. This illustrates the need for appropriate signal filtering during implementation of this method on hardware that the impedance measurements to achieve the highest levels of accuracy.

For a more comprehensive analysis, we created 10 noisy impedance datasets using random values for the Cole model parameters and applied the extraction process to each dataset. Both the reference and estimated parameters for all 10 cases are given in Table III. From these values, the estimated parameters have very small relative errors compared to the reference values. The execution time had very small variations for all 10 datasets, ranging from 104.0 ms to 107.2 ms with an average estimation time of 105.3 ms with standard deviation of 1.2 ms.

TABLE III
ESTIMATED VALUES OF COLE-IMPEDANCE MODEL USING NOISY DATASET (0.25% NOISE LEVEL).

Dataset No.		$R_\infty (\Omega)$	$R_1 (\Omega)$	$R_0 (\Omega)$	$C (\mu\text{F})$	α	$f_c (\text{kHz})$
1	Reference	680.00	760.00	1440.00	1.20	0.56	42.72
	Estimated	681.15	760.40	1441.55	1.21	0.56	42.31
2	Reference	280.00	96.00	376.00	1.90	0.72	24.83
	Estimated	279.98	96.09	376.07	1.90	0.72	24.80
3	Reference	816.14	251.09	1067.23	2.24	0.54	166.12
	Estimated	816.54	250.96	1067.50	2.25	0.54	164.65
4	Reference	210.00	458.57	668.57	0.71	0.59	128.65
	Estimated	209.50	458.81	668.31	0.71	0.59	130.12
5	Reference	170.56	596.34	766.90	1.50	0.61	15.83
	Estimated	169.50	595.13	764.63	1.49	0.61	16.03
6	Reference	542.96	996.17	1539.13	0.64	0.57	64.29
	Estimated	538.66	996.75	1535.41	0.63	0.57	65.60
7	Reference	652.62	734.41	1387.03	1.49	0.58	20.28
	Estimated	653.68	735.69	1389.37	1.50	0.58	20.04
8	Reference	689.91	191.68	881.59	1.37	0.65	51.38
	Estimated	690.95	191.90	882.85	1.39	0.65	50.06
9	Reference	525.92	239.28	765.20	2.32	0.64	19.45
	Estimated	525.25	238.84	764.09	2.30	0.64	19.75
10	Reference	107.73	269.25	376.98	3.25	0.67	5.87
	Estimated	107.54	267.58	375.12	3.24	0.67	5.91

The impact of higher noise levels on estimation accuracy was

also investigated. Using dataset No. 1 ($R_\infty=680.0 \Omega$, $R_1=760.0 \Omega$, $C=1.20 \mu\text{F}$ and $\alpha=0.56$) from Table III as the reference, datasets with 1%, 2%, 3% and 5% noise were generated. The parameters were extracted from these noisy datasets and are given in Table IV with simulations of the Cole impedance using these also given in Fig. 7. As it can be seen from Table IV, the estimated values of model parameters, except C , are very close the reference values for noise levels up to 2%. This supports that even in the presence of significant noise, this method is still able to effectively extract the Cole-impedance parameters from the dataset.

TABLE IV
ESTIMATED VALUES OF COLE-IMPEDANCE MODEL FOR DIFFERENT NOISE LEVELS.

Noise		$R_\infty (\Omega)$	$R_1 (\Omega)$	$R_0 (\Omega)$	$C (\mu\text{F})$	α	$f_c (\text{kHz})$
1%	Ref.	680.00	760.00	1440.0	1.20	0.56	42.72
	Est.	682.29	773.86	1456.16	1.39	0.55	39.86
	RE (%)	0.34%	1.82%	1.12%	15.60%	1.79%	6.69%
2%	Est.	685.22	789.02	1474.24	1.61	0.54	36.71
	RE (%)	0.77%	3.82%	2.38%	34.23%	3.57%	14.06%
	Est.	681.28	817.90	1499.19	2.09	0.52	33.51
3%	RE (%)	0.19%	7.62%	4.11%	73.83%	7.14%	21.57%
	Est.	676.81	868.86	1545.7	3.12	0.49	27.58
	RE (%)	0.47%	14.32%	7.34%	160.1%	12.5%	35.45%

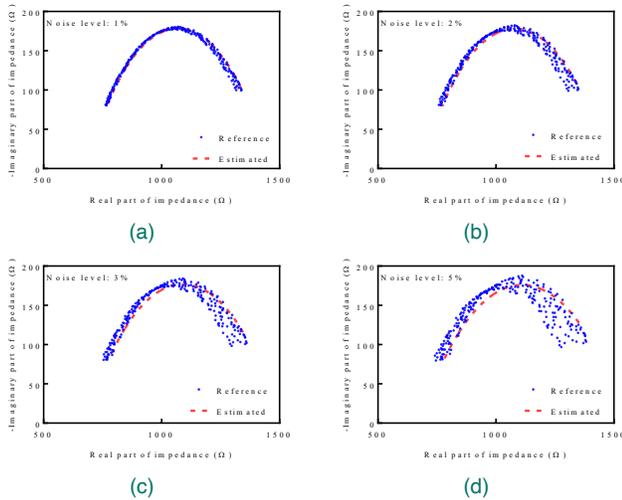


Fig. 7. The Nyquist plots of reference and estimated impedance for different noise levels (a) 1%, (b) 2%, (c) 3%, and (d) 5%.

B. Microcontroller-based implementation and comparison with literature

The development of low-cost microcontroller-based impedance measurement systems is gaining increased research interest [35] especially with the availability of commercial integrated circuits with impedance measurement functionality. Integrated circuits such as the AD5933 and AD9833 from Analog Devices support the realization of measurement systems that can measure impedances up to approximately 100 kHz (AD5933 [36]) and 1 MHz (AD9833 [37]). With these integrated circuits, it is possible to realize wearable and portable devices with impedance sensing functionality. Beyond measuring impedance, the integration of Cole-impedance extraction algorithms into these devices reduces the need for offline post-processing and larger data memory for storage of all raw data.

To validate the performance of the proposed method using

embedded hardware, the method was implemented on a microcontroller-platform based on the ATmega2560. This also enabled comparison with recent works that used the Raspberry Pi3 (RPi3) hardware as a platform to estimate the Cole-impedance parameters [18]. A comparison of the main specification parameters of our test platform with the RPi3 are shown in Table V. Moreover, the platform used in this work is similar in terms of resources to MSP430FR2433-based platforms used for validation of first-order optimization methods (gradient descent and coordinate descent) [38] and the STM32F407-based platform for multi-objective algorithm implementations [39].

TABLE V
COMPARISON OF MAIN SPECIFICATION PARAMETERS OF OUR WORK AND LITERATURE.

	[18], 2019	This work
Embedded Platform	Raspberry Pi 3	DFRduino Mega2560
Processor	ARM® Cortex®-A53, VideoCore	ATmega2560
Flash memory	Defined by memory card	256 kB
Clock speed	1.2 GHz	16 MHz
RAM	1 GB	8 kB
Operating system	Raspbian GNU/Linux 8	None
Specific software requirements	Python 3.4.2 and SciPy 0.14.0	None
Price	35.00 USD [40]	25.00 USD [41]

As it can be seen from Table V, the target platform for the proposed method has almost 30% lower price when compared to the RPi [18]. In addition to this lower price, there is no requirement for specific toolboxes or software packages (such as SciPy required in [21]), which is an advantage in terms of portability. The program code with the complete set of impedance data: arrays of ω , R and X with 256 elements and estimation method require just 6% of available 256 kB. Moreover, just 4731 of 8192 bytes of available RAM was occupied.

The performance of the parameter estimation using noisy data on the microcontroller hardware compared to the method in [18] is shown in Table VI. The estimates from the proposed method show very small differences when compared to those estimated by the RPi3 platform.

TABLE VI
ESTIMATED VALUES OF COLE-IMPEDANCE MODEL USING NOISY DATASET AND COMPARISON WITH LITERATURE.

	$R_\infty (\Omega)$	$R_1 (\Omega)$	$C (\mu\text{F})$	α	$f_c (\text{kHz})$
Reference values	84.40	39.20	2.31	0.747	41.16
[18], 2019	84.47	38.98	2.21	0.751	41.16
This work	84.23	39.06	2.20	0.75	41.99

Execution time of the proposed method ($t_{exe}=58.42 \text{ s}$) is approximately 1.88 times higher when compared to $t_{exe}=31.1 \text{ s}$ from [18]. That is not unexpected based on the higher clock speed of the platform in [18] (1.2 GHz) compared to this clock speed of the microcontroller platform used here (16 MHz). However, processing time with the proposed method can be significantly reduced if a two-step estimation is used. That is, in the first step a larger step of α is

used, for example 0.1. With this initial screening, the value of α_{initial} for the minimal error calculated with Eq. (10) is determined. In the second step, a finer step (for example, $\alpha=0.01$) is used in the neighboring range around α_{initial} : $\alpha_{\text{initial}}-0.1 \leq \alpha \leq \alpha_{\text{initial}}+0.1$ for more precise calculation of the minimal error with Eq. (10). Using this procedure, the same parameter values are estimated in 18.16 seconds, which is 1.71 times faster than $t_{\text{exe}}=31.1$ s from [18]. The proposed optimization of the estimation procedure is significant for microcontroller-based platforms, resulting in more than 3 times faster estimation (18.16 s < 58.42 s). This was expected because 101 iterations with an α -step of 0.01 were required in the range [0,1]. This was reduced to 32 using the two-step process (11 iterations in the initial screening from 0 to 1 with α -step of 0.1, and 21 iterations with α -step of 0.01 in the range from 0.7 to 0.9) are required.

When compared to previously reported microcontroller-based approaches for the Cole-impedance model parameter estimation [42], [43], our work advances the software estimation methods by eliminating the need for specific DC and high frequency measurement or numerical solving of the non-linear equation [15]. Further, the approach presented here also overcomes limitations of previous estimation methods that were limited to integer-order models [24], [25].

C. Parameter estimation using experimentally obtained bioimpedance

Experimental bioimpedance measurements were collected from a single participant after receiving informed consent using a commercial ImpediMed SFB7 device. This device collects 256 measurement points from 3 kHz to 1 MHz (logarithmic distribution, 100 points/dec). The participant was a 24 year old male (height: 173 cm and weight: 79 kg). The data collection procedures were approved by the regional ethics committee of Gothenburg with ethical approval number 274-11. The electrical impedance was measured between the participant's right hand and right foot using a 4-electrode configuration, as defined by ImpediMed SFB7 manual. In this configuration, one electrode pair is used for current delivery and the second pair is for voltage sensing. The device collected 10 consecutive measurements each requiring approximately 1 second to complete. The 10 datasets (M1-M10) were used for estimations with the proposed method and the BioImp software (version 2.3.4). The BioImp is software associated with the ImpediMed SFB7 device, primarily focused on the body composition analysis. Comparison of the estimated values of the parameters important for the body composition analysis (R_0 , R_∞ and f_c) between the two methods is given in Table VII. In the last row, the average value (μ) and standard deviation (σ) for all 10 estimations are given. As it can be seen, both estimation methods extracted very similar values of model parameters for all 10 measurements.

TABLE VII

COMPARISON OF THE ESTIMATED VALUES WITH THE PROPOSED METHOD AND BIOIMP SOFTWARE..

Measurement No.		R_∞ (Ω)	R_0 (Ω)	f_c (kHz)
M1	Bioimp	394.31	610.53	31.39
	This work	397.71	607.39	31.13
M2	Bioimp	400.17	616.11	32.45
	This work	400.92	619.50	31.35

M3	Bioimp	398.69	615.19	32.40
	This work	397.95	615.43	32.37
M4	Bioimp	398.42	615.45	32.46
	This work	397.88	615.62	32.39
M5	Bioimp	400.89	616.68	32.48
	This work	400.17	618.15	32.18
M6	Bioimp	399.88	616.40	32.52
	This work	400.99	623.07	30.20
M7	Bioimp	399.18	616.40	32.33
	This work	400.58	619.64	30.90
M8	Bioimp	399.14	615.32	32.38
	This work	400.49	618.93	30.92
M9	Bioimp	399.21	615.91	32.26
	This work	400.38	618.96	31.04
M10	Bioimp	398.97	616.10	32.20
	This work	400.07	618.83	31.08
$\mu \pm \sigma$	Bioimp	398.89 \pm 1.77	615.41 \pm 1.79	32.29 \pm 0.33
	This work	399.71 \pm 1.32	617.55 \pm 4.16	31.36 \pm 0.73

As an illustrative example, the comparison of the measured and estimated bioimpedances for dataset M1 is shown in Fig. 8.

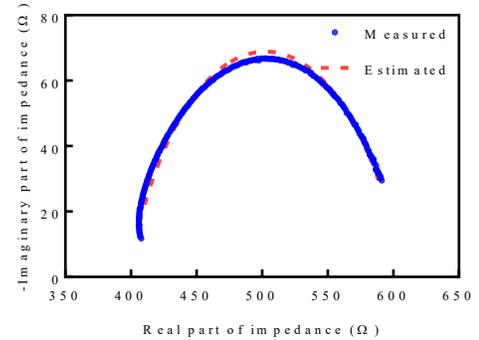


Fig. 8. The Nyquist plots of measured and estimated bioimpedance with the proposed method (dataset M1).

For an additional performance evaluation of the proposed method the mean absolute percentage error (MAPE) was calculated:

$$MAPE(\%) = \frac{1}{N} \sum_{i=1}^N \left| \frac{Z_{meas} - Z_{ref}}{Z_{ref}} \right| \times 100\% \quad (12)$$

where Z_{ref} is impedance modulus of the original impedance spectrum and Z_{meas} is the impedance modulus produced using the estimated parameters. Using (12) the obtained mean MAPE value for all 10 datasets is 0.196 \pm 0.054 %.

IV. CONCLUSION

The proposed low-complexity method for parameter estimation of Cole-impedance model, deployed on a low-cost embedded platform using an 8-bit microcontroller, was shown to be reliable solution for bioimpedance data processing. The estimation accuracy is comparable with more complex algorithms based on non-linear least squares approach, while required resources and price (25 USD < 35 USD [18]) are significantly lower.

The development of low-complexity algorithms for efficient bioimpedance data processing with embedded hardware is important for supporting portable and wearable sensing systems with significant resource constraints. The proposed algorithm enables on-site parameter estimation, which enables prompt decision making, reducing the time lag between measurement and actions. Moreover, the overall cost of the system is reduced,

which is very important goal in increase of number of portable devices for bioimpedance analysis (total body water, body mass index, etc.).

REFERENCES

- [1] P. Kassanos, "Bioimpedance sensors: A tutorial," *IEEE Sensors Journal*, 2021.
- [2] R. Kusche and M. Ryschka, "Combining bioimpedance and EMG measurements for reliable muscle contraction detection," *IEEE Sensors Journal*, vol. 19, no. 23, pp. 11687–11696, 2019.
- [3] J. Ferreira, I. Pau, K. Lindcrantz, and F. Seoane, "A handheld and textile-enabled bioimpedance system for ubiquitous body composition analysis. An initial functional validation," *IEEE journal of biomedical and health informatics*, vol. 21, no. 5, pp. 1224–1232, 2016.
- [4] D. Blanco-Almazan, W. Groenendaal, F. Catthoor, and R. Jane, "Wearable bioimpedance measurement for respiratory monitoring during inspiratory loading," *IEEE access*, vol. 7, pp. 89487–89496, 2019.
- [5] K. Sel, D. Osman, and R. Jafari, "Non-invasive cardiac and respiratory activity assessment from various human body locations using bioimpedance," *IEEE open journal of engineering in medicine and biology*, vol. 2, pp. 210–217, 2021.
- [6] S. Hersek *et al.*, "Wearable vector electrical bioimpedance system to assess knee joint health," *IEEE Transactions on Biomedical Engineering*, vol. 64, no. 10, pp. 2353–2360, 2016.
- [7] S. Mabrouk *et al.*, "Robust longitudinal ankle edema assessment using wearable bioimpedance spectroscopy," *IEEE Transactions on Biomedical Engineering*, vol. 67, no. 4, pp. 1019–1029, 2019.
- [8] O. I. Al-Surkhi and R. Y. Naser, "Detection of cell morphological changes of ischemic rabbit liver tissue using bioimpedance spectroscopy," *IEEE Transactions on NanoBioscience*, vol. 17, no. 4, pp. 402–408, 2018.
- [9] J. Li *et al.*, "An approach for noninvasive blood glucose monitoring based on bioimpedance difference considering blood volume pulsation," *IEEE Access*, vol. 6, pp. 51119–51129, 2018.
- [10] M. Ashoorirad, R. Baghbani, A. Fallah, N. Jooyan, and M. Gaffari, "A collagen thin film-based bioimpedance sensor for cell proliferation rate assessment," *IEEE Sensors Journal*, vol. 22, no. 1, pp. 61–67, 2021.
- [11] M. Simić, Z. Babić, V. Risojević, and G. M. Stojanović, "Non-iterative parameter estimation of the 2R-1C model suitable for low-cost embedded hardware," *Frontiers of Information Technology & Electronic Engineering*, vol. 21, no. 3, pp. 476–490, 2020.
- [12] F. Seoane, R. Buendía, and R. Gil-Pita, "Cole parameter estimation from electrical bioconductance spectroscopy measurements," in *2010 Annual International Conference of the IEEE Engineering in Medicine and Biology*, IEEE, 2010, pp. 3495–3498.
- [13] F. Shi, A. Steuer, J. Zhuang, and J. F. Kolb, "Bioimpedance Analysis of Epithelial Monolayers After Exposure to Nanosecond Pulsed Electric Fields," *IEEE Trans. Biomed. Eng.*, vol. 66, no. 7, pp. 2010–2021, Jul. 2019, doi: 10.1109/TBME.2018.2882299.
- [14] Tao Dai and A. Adler, "In Vivo Blood Characterization From Bioimpedance Spectroscopy of Blood Pooling," *IEEE Trans. Instrum. Meas.*, vol. 58, no. 11, pp. 3831–3838, Nov. 2009, doi: 10.1109/TIM.2009.2020836.
- [15] A. S. Elwakil and B. Maundy, "Extracting the Cole-Cole impedance model parameters without direct impedance measurement," *Electron. Lett.*, vol. 46, no. 20, p. 1367, 2010, doi: 10.1049/el.2010.1924.
- [16] K. S. Cole, "Permeability and impermeability of cell membranes for ions," in *Cold Spring Harbor symposia on quantitative biology*, Cold Spring Harbor Laboratory Press, 1940, pp. 110–122.
- [17] I. Podlubny, *Fractional Differential Equations*, 1st ed., vol. 198. 1st ed., 1998.
- [18] T. J. Freeborn, "Performance evaluation of raspberry Pi platform for bioimpedance analysis using least squares optimization," *Personal and Ubiquitous Computing*, vol. 23, no. 2, pp. 279–285, 2019.
- [19] F. Zhang *et al.*, "A novel method for estimating the fractional Cole impedance model using single-frequency DC-biased sinusoidal excitation," *Circuits, Systems, and Signal Processing*, vol. 40, no. 2, pp. 543–558, 2021.
- [20] D. A. Yousri, A. M. AbdelAty, L. A. Said, A. AboBakr, and A. G. Radwan, "Biological inspired optimization algorithms for cole-impedance parameters identification," *AEU-International Journal of Electronics and Communications*, vol. 78, pp. 79–89, 2017.
- [21] R. G. Ramírez-Chavarria, G. Quintana-Carapia, M. I. Müller, R. Mattila, D. Matatagui, and C. Sánchez-Pérez, "Bioimpedance Parameter Estimation using Fast Spectral Measurements and Regularization," *IFAC-PapersOnLine*, vol. 51, no. 15, pp. 521–526, 2018, doi: 10.1016/j.ifacol.2018.09.198.
- [22] Y. Yang, W. Ni, Q. Sun, H. Wen, and Z. Teng, "Improved Cole parameter extraction based on the least absolute deviation method," *Physiological measurement*, vol. 34, no. 10, p. 1239, 2013.
- [23] F. Zhang, Z. Teng, S. Rutkove, Y. Yang, and J. Li, "A Simplified Time-Domain Fitting Method Based on Fractional Operational Matrix for Cole Parameter Estimation," *IEEE Trans. Instrum. Meas.*, vol. 69, no. 4, pp. 1566–1575, Apr. 2020, doi: 10.1109/TIM.2019.2912592.
- [24] M. Simić, A. K. Stavrakis, and G. M. Stojanović, "A Low-Complexity Method for Parameter Estimation of the Simplified Randles Circuit With Experimental Verification," *IEEE Sensors Journal*, vol. 21, no. 21, pp. 24209–24217, 2021.
- [25] M. Simic, A. K. Stavrakis, V. Jeoti, and G. M. Stojanovic, "A Randles Circuit Parameter Estimation of Li-Ion Batteries With Embedded Hardware," *IEEE Trans. Instrum. Meas.*, vol. 71, pp. 1–12, 2022, doi: 10.1109/TIM.2022.3183661.
- [26] U. Kyle, "Bioelectrical impedance analysis?part I: review of principles and methods," *Clinical Nutrition*, vol. 23, no. 5, pp. 1226–1243, Oct. 2004, doi: 10.1016/j.clnu.2004.06.004.
- [27] L. C. Ward and B. H. Cornish, "Bioelectrical impedance analysis at the characteristic frequency," *Nutrition*, vol. 23, no. 1, p. 96, Jan. 2007, doi: 10.1016/j.nut.2006.09.003.
- [28] T. J. Freeborn and S. Critcher, "Cole-Impedance Model Representations of Right-Side Segmental Arm, Leg, and Full-Body Bioimpedances of Healthy Adults: Comparison of Fractional-Order," *Fractal Fract*, vol. 5, no. 1, p. 13, Jan. 2021, doi: 10.3390/fractalfract5010013.
- [29] H. Sato *et al.*, "Effectiveness of impedance parameters for muscle quality evaluation in healthy men," *J Physiol Sci*, vol. 70, no. 1, p. 53, Dec. 2020, doi: 10.1186/s12576-020-00780-z.
- [30] A. De Lorenzo, A. Andreoli, J. Matthie, and P. Withers, "Predicting body cell mass with bioimpedance by using theoretical methods: a technological review," *Journal of Applied Physiology*, vol. 82, no. 5, pp. 1542–1558, May 1997, doi: 10.1152/jappl.1997.82.5.1542.
- [31] H. Schulz, D. Teske, D. Penven, and J. Tomczak, "Fat-free mass from two prediction equations for bioelectrical impedance analysis in a large German population compared with values in Swiss and American adults: Reasons for a biadata project," *Nutrition*, vol. 22, no. 9, pp. 973–975, Sep. 2006, doi: 10.1016/j.nut.2006.04.007.
- [32] T. Freeborn and B. Fu, "Fatigue-Induced Cole Electrical Impedance Model Changes of Biceps Tissue Bioimpedance," *Fractal Fract*, vol. 2, no. 4, p. 27, Oct. 2018, doi: 10.3390/fractalfract2040027.
- [33] B. Fu and T. J. Freeborn, "Cole-impedance parameters representing biceps tissue bioimpedance in healthy adults and their alterations following eccentric exercise," *Journal of Advanced Research*, vol. 25, pp. 285–293, Sep. 2020, doi: 10.1016/j.jare.2020.05.016.
- [34] N. López, D. García, C. A. González-Correa, and C. A. González-Díaz, "Estimation of Cole Parameters in ex-vivo tissues as a function of degradation time," *J. Phys.: Conf. Ser.*, vol. 2008, no. 1, p. 012011, Aug. 2021, doi: 10.1088/1742-6596/2008/1/012011.
- [35] A. Yufera and A. Rueda, "A method for bioimpedance measure with four- and two-electrode sensor systems," in *2008 30th Annual International Conference of the IEEE Engineering in Medicine and Biology Society*, Vancouver, BC: IEEE, Aug. 2008, pp. 2318–2321. doi: 10.1109/IEMBS.2008.4649662.
- [36] M. Simic, "Realization of complex impedance measurement system based on the integrated circuit AD5933," in *2013 21st Telecommunications Forum Telfor (TELFOR)*, IEEE, 2013, pp. 573–576.
- [37] Y. Yang, J. Wang, G. Yu, F. Niu, and P. He, "Design and preliminary evaluation of a portable device for the measurement of bioimpedance spectroscopy," *Physiol. Meas.*, vol. 27, no. 12, pp. 1293–1310, Dec. 2006, doi: 10.1088/0967-3334/27/12/004.
- [38] X. Zhang, J. Sartori, M. Hong, and S. Dhople, "Implementing First-order Optimization Methods: Algorithmic Considerations and Bespoke Microcontrollers," in *2019 53rd Asilomar Conference on Signals, Systems, and Computers*, Pacific Grove, CA, USA: IEEE, Nov. 2019, pp. 296–300. doi: 10.1109/IEEECONF44664.2019.9048681.

- [39] P. Henriquede Oliveira Santos *et al.*, “Multi-Objective Genetic Algorithm Implemented on a STM32F Microcontroller,” in *2018 IEEE Congress on Evolutionary Computation (CEC)*, Rio de Janeiro: IEEE, Jul. 2018, pp. 1–7. doi: 10.1109/CEC.2018.8477938.
- [40] “Digikey- Raspberry Pi3.”
<https://www.digikey.be/en/products/detail/raspberry-pi/RASPBERRY-PI-3/6152799>, Accessed on 15th June 2022 (accessed Jun. 15, 2022).
- [41] “Digikey-MEGA2560.” Accessed: Jun. 15, 2022. [Online]. Available: <https://www.digikey.be/en/products/detail/dfrobot/DFR0191/6579339>
- [42] H. Solmaz, Y. Ülgen, and M. Tümer, “Design of A Microcontroller Based Cole-Cole Impedance Meter for Testing Biological Tissues,” in *World Congress on Medical Physics and Biomedical Engineering, September 7 - 12, 2009, Munich, Germany*, O. Dössel and W. C. Schlegel, Eds., in IFMBE Proceedings, vol. 25/7. Berlin, Heidelberg: Springer Berlin Heidelberg, 2009, pp. 488–491. doi: 10.1007/978-3-642-03885-3_135.
- [43] P. Ibba, G. Cantarella, B. D. Abera, L. Petti, A. Falco, and P. Lugli, “Selection of Cole Model Bio-Impedance Parameters for the Estimation of the Ageing Evolution of Apples,” in *17th International Conference on Electrical Bioimpedance*, P. Bertemes-Filho, Ed., in IFMBE Proceedings, vol. 72. Singapore: Springer Singapore, 2020, pp. 25–32. doi: 10.1007/978-981-13-3498-6_4.